lation suggesting that the stable conformation of the radical is planar,[9] and thus it might be possible to assert that the circumstances of the canal complex make the nonplanar structure stable. If the above assertion is true, it follows that the most stable conformation (S) is pyramidal and the next stable one (U) is planar as in the MINDO calculation. These two structures cannot exist at the same time unless unreasonable structures are assumed. However, if a pyramidal conformation is the most stable at the equilibrium state, it is reasonable to suppose that the next stable one is its inverse conformation. This is the present case.

In conclusion, the structure of the methylcyclohexyl radical is pyramidal at the equilibrium state and the angle of CCC is about 117°. At the low temperature, there are two nonplanar conformations and the radical does the umbrella inversion between these conformations. The existence of the wall of thiourea makes it possible to observe this inversion. At the higher temperatures, this umbrella inversion occurs rapidly and the radical can be thought to be planar.

Registry No. $NH_2C(=S)NH_2$, 62-56-6; methylcyclohexane, 108-87-2; methylcyclohexyl radical, 16998-65-5.

(9) Igual, J. *THEOCHEM* **1985**, *121*, 221.

Electronic Relaxation of $Xe_2^+Cl^-$ in Solid and Liquid Xenon

Lawrence Wiedeman, Mario E. Fajardo, and V. A. Apkarian*

Department of Chemistry, University of California, Irvine, California 92717 *(Received: June 4, 1987)*

Emission spectra of $Xe_2^+Cl^-$ are presented in gas, liquid, and solid xenon. Lifetimes have been measured in both liquid and solid xenon between 12 and 240 K. $Xe_2^+Cl^-(4^2\Gamma)$ relaxes radiatively in solid xenon from 12 to 160 K. The radiative lifetime shows only a minor temperature dependence: 225 ± 2 ns at 12 K and 240 ± 10 ns at 160 K. The exciplex is quenched in liquid xenon by diffusion-controlled encounters with Cl_2. The efficiency of this nonradiative relaxation is ~0.1 per encounter. Neither xenon nor atomic Cl is effective in relaxing the exciplex in the liquid phase.

Introduction

Rare gas solids and liquids are prototypical media for the investigation of condensed-phase dynamics. Matrix isolation techniques have provided a wealth of information on the disposition of molecular electronic excitations in atomic solids.[1] The liquid-phase counterpart of such studies is fairly limited, although they are arguably more relevant to chemical dynamics.[2] In this report we describe the electronic relaxation of the lowest energy xenon chloride exciplex, $Xe_2^+Cl^-(4^2\Gamma)$, photogenerated in Cl_2:Xe solutions. It is shown that the solvent is ineffective in relaxing the exciplex and that the main nonradiative relaxation channel is due to diffusion-controlled encounters between the exciplex and Cl_2 molecules. In the case of solids, the exciplex relaxes by radiation.

In addition to the fundamental interests, these studies are motivated by practical considerations. Rare gas halides can be efficiently photogenerated in both rare gas solids[3-6] and liquids.[7-9] The photodynamics of these condensed-phase exciplexes can be described along the lines of ideal four-level lasers. We have demonstrated this by gain measurements on the $Xe_2^+Cl^-$ transitions in both solid[6] and liquid[9] xenon. Laser action in liquid argon had previously been demonstrated by both optical[8] and electron beam[10] pumping techniques. The liquids, due to their nonscattering properties, are the preferred media for such applications. An understanding of the mechanisms and rates of relaxation of the exciplexes in these dense media is essential for the intelligent design of such systems.

As a convenient means of generating rare gas halides in condensed media, we rely on two-photon cooperative absorption induced charge transfer in X_2:Rg mixtures (X_2 = molecular halogen, Rg = rare gas). The quantum electrodynamical formulation of generalized cooperative two-photon absorption processes and a discussion of their efficiency in condensed media has recently been presented in a series of papers by Andrews et al.[11] In the case of charge-transfer transitions, the process can be regarded as two-photon-induced harpooning, which in the case of Cl_2:Xe mixtures can be summarized as:

$$Xe + Cl_2 + 2h\nu \rightarrow Xe^+Cl_2^- \rightarrow Xe^+Cl^- + Cl \qquad (1)$$

In a large xenon background, the diatomic exciplex is reactively quenched to yield the lowest energy molecular exciplex, namely the triatomic $Xe_2^+Cl^-(4^2\Gamma)$ state:

$$Xe^+Cl^- + 2Xe \rightarrow Xe_2^+Cl^-(4^2\Gamma) + Xe \qquad (2)$$

The detailed analysis of this mechanism in the gas phase has been discussed by Setser and co-workers.[12] Its application and generalization to condensed phases is presented in a separate report by us.[13] The mechanism is efficient in both solids and liquids. The major difference between the two media is that in low-temperature solids (10–50 K), the halogen is permanently dissociated while in the case of liquids and high-temperature solids the halogen atoms recombine between excitation pulses.

(1) Brus, L. E.; Bondybey, V. E. In *Radiationless Transitions*; Lin, S. H., Ed.; Academic: New York, 1980.
(2) Schwentner, N.; Koch, E.-E.; Jortner, J., Eds.; *Electronic Excitations in Condensed Rare Gases*; Springer Tracts in Modern Physics 107; Springer-Verlag: New York, 1985.
(3) Ault, B. S.; Andrews, L. *J. Chem. Phys.* **1976**, *10*, 4192.
(4) Goodman, J.; Brus, L. E. *J. Chem. Phys.* **1976**, *65*, 3808; *J. Chem. Phys.* **1977**, *67*, 1482.
(5) Fajardo, M. E.; Apkarian, V. A. *J. Chem. Phys.* **1986**, *85*, 5660.
(6) Fajardo, M. E.; Apkarian, V. A. *Chem. Phys. Lett.* **1987**, *134*, 51.
(7) Jara, H.; Pummer, H.; Egger, H.; Rhodes, C. K. *Phys. Rev. B: Condens. Matter* **1984**, *30*, 1.
(8) Shahid, M.; Jara, H.; Pummer, H.; Egger, H.; Rhodes, C. K. *Opt. Lett.* **1985**, *10*, 448.
(9) Wiedeman, L.; Fajardo, M. E.; Apkarian, V. A. *Chem. Phys. Lett.* **1987**, *134*, 55.
(10) Loree, T. R.; Showalter, R. R.; Johnson, T. M.; Birmingham, B. S.; Hughes, W. M. *Opt. Lett.* **1986**, *11*, 510.
(11) Andrews, D. L.; Harlow, M. J. *J. Chem. Phys.* **1983**, *78* 1088; *J. Chem. Phys.* **1984**, *80*, 4753.
(12) Yu, Y. C.; Setser, D. W.; Horiguchi, H. *J. Phys. Chem.* **1983**, *87*, 2209. Setser, D. W.; Ku, J. In *Photophysics and Photochemistry above 6 eV*; (Elsevier: New York, 1985); p 621.
(13) Fajardo, M. E.; Wiedeman, L.; Apkarian, V. A. *Proceedings of IQEC* Baltimore, 1987; Post Deadline Report, PD-16; also manuscript in preparation.

0022-3654/88/2092-0342$01.50/0

The formation of the triatomic exciplex is followed by monitoring its characteristically broad emission. The emission undergoes a shift both as a function of temperature and as a function of density of the polarizable medium. In rare gas matrices, the triatomic emission is centered at 570 nm as compared to 485 nm in the gas phase at atmospheric pressures. However, unlike the diatomic exciplexes, whose radiative lifetimes and line shifts are directly correlated with the polarizability of the media, in the case of $Xe_2^+Cl^-$ the same emission is observed in solid Ar, Kr, and Xe hosts and the radiative lifetime is similar to that observed in the gas phase.[5] Due to this anomalous behavior and the large spectral shift, the identification of the emitter as the molecular triatomic exciplex has been the subject of concern and theoretical scrutiny.[14] By continuously monitoring the emission band across phase lines, the localized molecular nature of the charge-transfer complexes in all phases can be established. Such spectra have been obtained and will be presented prior to discussion of the relaxation data.

Experimental Section

A detailed description of the experimental apparatus and methodology can be found in ref 5 and 9. The low-temperature, 12–50 K, solid-state studies are conducted by standard matrix isolation techniques. The gas, liquid, and high-temperature solids are investigated in a high-pressure cryocell attached to the cryotip of a liquid helium cryostat. The design of the cell can be found in ref 9. Due to the large heat capacity of the cell and the use of liquid nitrogen as cryogen, the lowest accessible temperature in these studies is 140 K. The reported temperatures are corrected by reference to the temperature at thermal arrest during freezing. The reproducibility of these temperatures is within 1 K. The cryocell has a volume of 0.8 cm^3. It is attached to the room temperature gas-handling manifold through $^1/_{16}$-in. o.d. stainless steel tubulation. The vapor pressure of the liquid is continuously monitored during the experiment. The dead volume of the gauge and tubulation leading to the liquid cell is 16 cm^3.

The experimental procedure is as follows: (a) A premixed gas sample of Cl_2:Xe is introduced in the cell, and its pressure is measured at room temperature. (b) The cell temperature is lowered to a temperature below the critical point of xenon (289.8 K). (c) Sufficient xenon is added to fill the entire cell with liquid, and the system is isolated from the xenon reservoir. (d) Lifetimes are measured as a function of temperature. To avoid changes in mole fractions, the investigation is halted as soon as a meniscus is observed. The highest temperature of the study then corresponds to the temperature at which the cell was filled, ~245 K in the present work. (e) Near the melting point, in the solid phase, measurements are made upon completion of freezing during cooldown; in the liquid phase, measurements are made during the warm-up cycle and upon completion of melting. Nonscattering, inclusion crystals of high optical quality are occasionally formed by this method. It was noted that during the slow freezing an effective zone refining takes place, such that the halogen molecules are preferentially concentrated in the liquid phase. This is in part responsible for a decrease in emission intensity upon freezing of a given solution. The same effect is also observed in Br_2:Xe solutions. In the latter case, the segregation could be visually verified by observing the differential coloration of the solid vs its melt.

The concentrations are obtained from the measured Cl_2 pressure and the known temperature-dependent density of liquid xenon.[15] It is assumed that the chlorine is entirely dissolved in the liquid phase. The error made by this assumption is small in the range of temperatures at which the liquid-phase studies are conducted (160–250 K). The percent error, Δx (%), made in mole fractions can be estimated by assuming the system obeys Raoult's law as:

$$\Delta x\ (\%) = 10^5 \frac{V_g}{V_l} \frac{P^0(T)}{RT} \frac{M}{\rho(T)} \qquad (3)$$

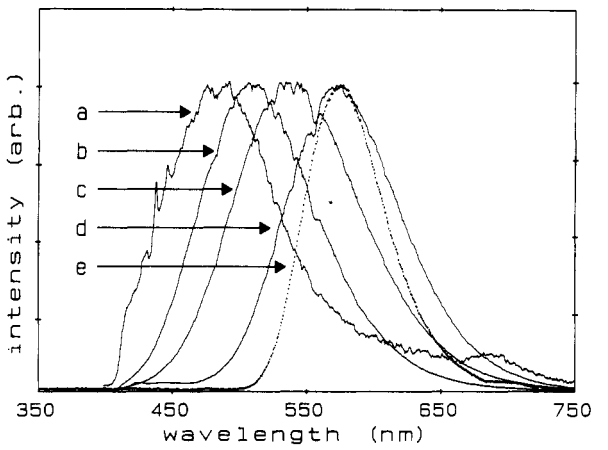

Figure 1. Representative $Xe_2^+Cl^-(4^2\Gamma)$ emission spectra shown in gas, liquid, and solid xenon. In all cases, the spectra were obtained by 308-nm excitation of Cl_2:Xe mixtures. (a) Gas phase, Cl_2:Xe = 1:500, P = .66 atm, T = 260 K; (b) gas phase, Cl_2:Xe = 1:23 000, P = 30.1 atm, T = 264 K; (c) liquid phase, Cl_2:Xe = 1:300 000, T = 260 K, density of the liquid = 2.03 g cm^{-3}, which is equivalent to 330 atm of gas; (d) liquid phase, Cl_2:Xe = 1:350 000, T = 163 K; (e) solid, original concentration of 0.1% Cl_2, T = 12 K.

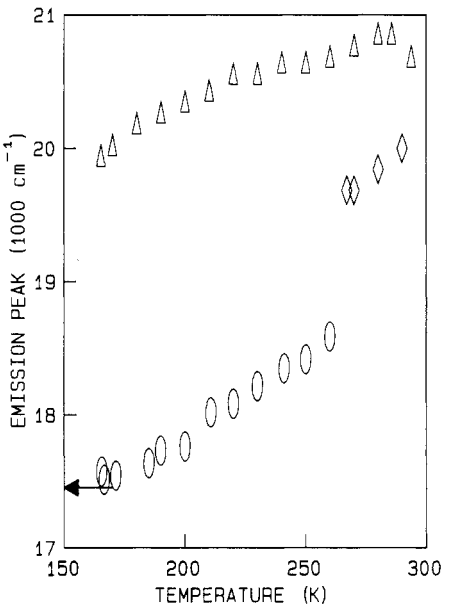

Figure 2. $Xe_2^+Cl^-$ emission peak centers in gas and liquid xenon plotted versus temperature. The arrow represents the peak center in solid xenon at 12 K. Triangles: gas phase, total pressure = 0.66 atm. Diamonds: gas phase, total pressure = 30.1 atm. Ovals: liquid phase.

in which V_g and V_l are the volumes of the gas and liquid, respectively, M is the atomic mass of xenon, ρ is the saturated liquid density of xenon obtained from ref 15, and $P^0(T)$ is the temperature-dependent vapor pressure[16] of Cl_2:

$$\log P^0 = \frac{-29293 \times 0.05223}{T} + 9.95 \qquad (4)$$

The largest error made is 3.3% at 250 K (1.3% at 230 K). These errors are well within the errors associated with lifetime measurements and hence are ignored.

The emission spectra were recorded with an optical multichannel analyzer with an array of 730 intensified diodes (EG&G, PAR). The lifetime measurements were performed with a PMT (Hamamatsu R666), followed by a 300-MHz preamplifier (Phillips 6950), and a boxcar equipped with a scanning gate (SRS SR250).

(14) Last, I.; George, T. F. *J. Chem. Phys.* **1987**, *86*, 3787. Last, I.; George, T. F.; Fajardo, M. E.; Apkarian, V. A., submitted for publication in *J. Chem. Phys.*

(15) Theeuwees, F.; Bearman, R. J. *J. Chem. Thermodyn.* **1970**, *2*, 507.

(16) *Handbook of Chemistry and Physics*, 55th ed.; Chemical Rubber Co.: Boca Raton, FL, 1974.

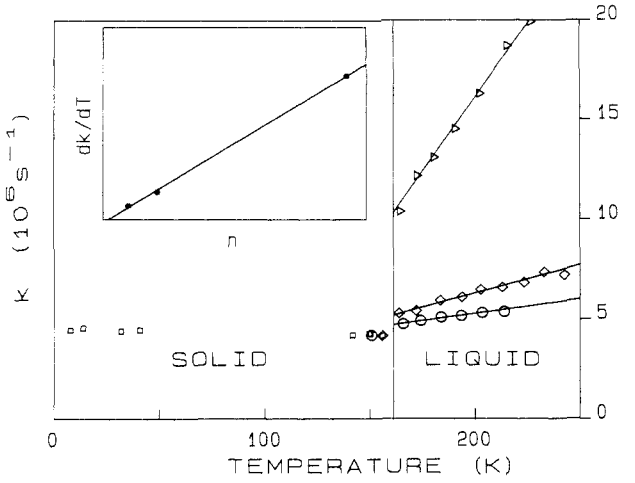

Figure 3. Relaxation rates, k, of $Xe_2^+Cl^-$ in solid and liquid xenon shown as a function of temperature. The vertical line is drawn at the melting point of xenon. The solid-phase data (squares) between 12 and 50 K pertain to matrices, while those between 140 and 160 K are from frozen liquid solutions of different concentrations. The liquid-phase data are for three different concentrations: triangles, diamonds, and circles correspond to 4.6, 1.0, and 0.475 mM solutions, respectively. Also shown are the best fit lines to the k vs T plots, and in the inset, the slopes of the best fit lines are plotted versus the Cl_2 number densities. The x axis of the inset is identical with that of Figure 4b.

The Cl_2 gas was purchased with a nominal purity of 99.0% and further purified by several trap to trap distillations. Xenon gas of 99.999% purity purchased from Spectra Gases was used without further purification.

Results and Discussion

A. Emission Spectra. Emission spectra obtained by 308-nm excitation of Cl_2:Xe mixtures in gas, liquid, and solid xenon are shown in Figure 1. The wavelengths of the emission maxima are plotted in Figure 2 as a function of temperature. The data are from two different gas mixtures—total pressures of 0.66 and 30.1 atm—and from a liquid solution. In the low-pressure gas mix, and at room temperature, the emission is centered at 485 nm. This emission is well known to be due to $Xe_2^+Cl^-(4^2\Gamma)$.[17] The emission band narrows asymmetrically, and the maximum undergoes a red shift as a function of temperature. This shift can be ascribed to the lowering of the vibrational temperature of the exciplex. Since the transition terminates on a repulsive ground state, the band should narrow asymmetrically. The density dependence of the line shift can be clearly discerned from the data at ~260 K, for gas at 0.66 atm, gas at 30 atm, and liquid (equivalent to 330 atm of gas). This shift can be rationalized as due to the ionic-covalent nature of the transition. Due to the large dipole of the upper state, 12 D, the exciplex-state energy is lowered by polarization of the medium while the covalent repulsive surface is unaffected. The observed red shift in the liquid phase is then due to the combination of vibrational cooling and increased bulk polarizability (or density) of the compressible liquid. As discussed previously, classical models of solvent-shift theories can adequately explain these shifts.[9] It is important to note that the emission line center does not undergo a perceptible shift upon freezing and in the solid phase from 160 to 10 K. This is despite the fact that the density of the solid increases by ~10% in this range. We will return to this point after discussing the radiative lifetimes. The important conclusion to be made from these data is that the condensed-phase emissions can be directly and continuously correlated to the well-known triatomic exciplex, $Xe_2^+Cl^-(4^2\Gamma)$.

B. Lifetimes. The laser-induced fluorescence of $Xe_2^+Cl^-$ in both solid and liquid xenon decays exponentially.[5,9] A compilation of the relaxation rates, inverse lifetimes, is presented in Figure 3 as a function of temperature and for different Cl_2:Xe concentrations. The solid- and liquid-phase data are separated by the vertical line drawn at the melting point. The important features to note are (a) the observed lifetimes are nearly constant in the solid phase from 12 to 160 K, independent of concentration, (b) the observed lifetimes in the liquid phase show a linear dependence on both temperature and concentration, and (c) for a solution of a given concentration, an abrupt change in lifetime is observed across the solid–liquid-phase line.

i. Radiative Decay. The data in the 12–50 K range of Figure 3 are obtained from our earlier matrix studies in which it was established that the relaxation is radiative and independent of temperature or concentration.[5] The lifetime at 12 K, 225 ± 2 ns, is the result of 12 separate measurements in matrices of different preparation.

The data in the 140–160 K range pertain to solids formed by slow freezing of Cl_2:Xe solutions in the cryocell. On the basis of the increased density, hence index of refraction, of solid xenon between 160 and 10 K, a reduction in radiative lifetime is to be expected according to the commonly accepted relation:[18]

$$\frac{\tau(n)}{\tau(n')} = \frac{n'(n^2+2)^2}{n(n^2+2)^2} = 0.89 \qquad (5)$$

in which n and n' are the indices of refraction at 10 and 160 K respectively: n(160 K) = 2.060 and n'(10 K) = 2.227 as calculated from the known densities of crystalline xenon.[19] The observed ratio $\tau(12)/\tau(160)$ is 0.94 ± 0.04, consistent with the above prediction particularly in view of the fact that xenon matrices formed by vapor deposition of xenon on a cold surface are far from being crystalline (the predicted reduction in lifetime is based on the density of crystalline xenon). It is worth noting that eq 5 has previously proven valid in relating the diatomic $Xe^+Cl^-(C)$ lifetimes in solid argon and krypton to that of the gas phase.[5] The absence of any concentration dependence and the mild temperature dependence—predictable based on changes in the dielectric constant of the medium alone—establish that $Xe_2^+Cl^-$ relaxes radiatively in solid xenon at all temperatures. It is then determined experimentally that the radiative relaxation rate has a temperature dependence of $\Delta(1/\tau_r)/\Delta T = -2\ (\pm 1) \times 10^3\ s^{-1}\ K^{-1}$.

It is important to note that the radiative lifetime of 240 ± 10 ns at 160 K in solid xenon is, within experimental error, the same as that reported for the gas phase,[20] 245 ± 10 ns. The argument used above for the solids cannot then be applied to the range between the melting point and the low-pressure gas. Another difference between the two cases is that a large red shift is observed in the latter range of densities, while the line shift in the solids between 160 and 12 K is negligible. Then the change in oscillator strength of the transition is reflected in the reduction of lifetimes in the solid, while in the liquid and gas phases, it is reflected in the shift of the emission line center. While the magnitude of these shifts can be justified by simple solvent-shift theories, the details cannot. Specific solvent–solute interactions should be considered to account for the details. In particular the softening of the Coulombic exciplex potential and the associated shift of the potential minimum to longer intermolecular distances should be considered. Such a treatment, while in principle possible, is beyond the scope of the present report. For our present purposes, suffice to conclude that the radiative lifetime undergoes a minor change in the range between the melting point and room temperature gaseous xenon.

ii. Nonradiative Decay. The relaxation data above 161 K pertain to liquid Cl_2:Xe solutions at three different concentrations: 4.6, 1.0, and 0.475 mM. The relaxation rates increase as a function of temperature and Cl_2 concentration. With the exception of the discontinuity at the freezing point, the dependence of relaxation rates on temperature is essentially linear in the studied range, with slopes directly proportional to the Cl_2 concentration. In the most dilute solution, the relaxation time approaches the

(17) Huestis, D. L.; Marowsky, G.; Tittel, F. K. In *Excimer Lasers*; Rhodes, C. K., Ed.; Topics in Applied Physics 30; Springer-Verlag: New York, 1984; Chapter 6.

(18) Fulton, R. L. *J. Chem. Phys.* **1974**, *61*, 4141.

(19) Klein, M. L.; Venables, J. A., Eds. *Rare Gas Solids*; Academic: New York, 1977; Vol. II, p 381.

solid-phase values and hence is dominated by radiation. The abrupt change across the solid–liquid-phase line implies that, upon freezing, the relaxation becomes radiative. The dependence of the nonradiative contribution to relaxation upon Cl_2 concentrations and its elimination upon freezing are clear indications that the relaxation is diffusion controlled in the liquid phase. Therefore, the nonradiative relaxation is dominated by $Xe_2^+Cl^-$–Cl_2 encounters. The efficiency of this process in the gas phase is known to be nearly gas kinetic.[20-22] If the same efficiency is maintained in the liquid phase, then the liquid-phase deactivation should be strictly diffusion limited.

The observed fluorescence decay rate can be treated as the sum of radiative and nonradiative terms. For a diffusion-controlled nonradiative relaxation, the overall decay rate, k, can be expressed as:

$$k = \frac{1}{\tau} = \frac{1}{\tau_r} + \frac{1}{\tau_{nr}} \tag{6a}$$

$$= \frac{1}{\tau_r} + 4\pi r D n \tag{6b}$$

in which τ is the observed lifetime, τ_r is the radiative lifetime, r is the relaxative collision radius, n is the Cl_2 number density, and D is the diffusion constant of Cl_2 in liquid xenon. The assumption of pseudo-first-order kinetics and the neglect of the exciplex diffusion rates are made in eq 6b. We will first present an approximate treatment of the data, which is useful since it requires no additional information about the properties of the liquid.

It is known that diffusion in van der Waals liquids is well approximated by the Stokes–Einstein relation in the slip limit:[23] $D = k_B T/4\pi\eta a$ (k_B = Boltzmann constant; η = viscosity; a = radius of diffuser—Cl_2 in the present case). The observed relaxation rate can then be recast in the form:

$$k = \frac{1}{\tau} = \frac{1}{\tau_r} + \frac{r}{a}\frac{nk_BT}{\eta} \tag{7}$$

Since the experiments are conducted along the liquid–vapor coexistence line, we may expect that the variation in η in the range of studied temperatures is minor. Then eq 7 explains both the linear temperature and the linear concentration dependence observed in the data. The Eyring model for viscosity yields a useful approximation:[24]

$$\eta = h\left(\frac{\rho(T)}{M}\right)_{Xe} e^{3.8T_B/T} \tag{8}$$

The viscosity according to eq 8 can be exactly evaluated from the known temperature-dependent saturated liquid density of xenon.[15] However, to a first approximation, if we assume η to be a constant given by its value at the boiling point T_B = 167 K, $\eta(T_B) = 4 \times 10^{-3}$ erg s cm^{-3}, the temperature dependence of the relaxation rate can be expressed as:

$$\left(\frac{dk}{dT}\right)_{T_B} = \frac{k_B}{\eta(T_B)}\frac{rn}{a} \tag{9}$$

The best fit lines to the k vs T plots are shown in Figure 3. In the inset, the slopes are plotted versus n. From the slope of dk/dT vs n, the ratio of relaxational radius to that of diffuser radius, r/a, can be obtained directly as 1.6 ± 0.3. While this is a reasonable value and would imply a deactivation probability of unity per exciplex–Cl_2 encounter, due to our neglect of the explicit temperature dependence of η, the derived value is an overestimate. A more exact treatment will be presented below. This approximate treatment is useful for making several conclusions:

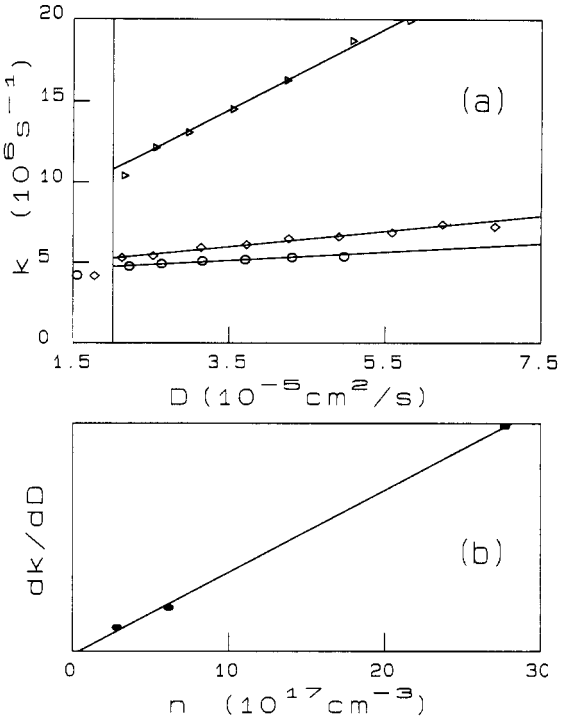

Figure 4. (a) Plot of $Xe_2^+Cl^-$ relaxation rates as a function of diffusion constant D. D was calculated from the reduced equation of self-diffusion in liquid rate gases. The vertical line is drawn at the melting point of xenon. Diffusion constants near and below the melting point are not meaningful. The data to the left of the mp line represent relaxation rates of the frozen solutions. The data points are the same as those in Figure 3. (b) The slopes of the best fit lines in (a), dk/dD, are plotted versus the number density of Cl_2. From the slope of the line, the quenching radius is obtained as r = 0.7 ± 0.1 Å.

(a) The absence of a positive y intercept in the plot of dk/dT vs n implies that the solvent does not deactivate the exciplex.

(b) The presence of a negative y intercept implies that the fluorescence decay has a contribution independent of Cl_2 concentration with inverse temperature dependence. The intercept of the best fit line is -3×10^3 s^{-1} K^{-1}. This is entirely accountable by the temperature dependence of radiative lifetimes, which was determined from the solid-state data to be -2 (±1) $\times 10^3$ s^{-1} K^{-1}.

(c) An alternate interpretation of (b) is that there is a nonzero x intercept in the dk/dT vs n plot. This would be the case if the liquid contained a soluble impurity. The x intercept would then correspond to an impurity level of 4 ppm—well within the impurity level specified by the manufacturer. The correct picture most certainly contains contributions from both (b) and (c).

(d) There is little significance in the intercepts of the k vs T plot at the melting point, other than the fact that the diffusion model cannot account for processes near phase transitions.

A more exact treatment of the data can be achieved by taking into account the explicit temperature dependence of η. To avoid the implicit approximations made in eq 5, we present an alternate treatment based on the known behavior of self-diffusion in van der Waals liquids. The results obtained by either approach are quantitatively the same. Naghizadeh and Rice have studied self-diffusion in rare gas liquids by monitoring the diffusion of tracer radioactive isotopes.[25] Self-diffusion in all rare gases can be expressed in terms of reduced parameters:

$$\log \sim\tilde{D} = 0.05 + 0.07\tilde{p} - (1/\tilde{T})(1.04 + 0.1\tilde{p}) \tag{10}$$

in which $\tilde{D} = (m/\epsilon\sigma^2)^{1/2}D$, $\tilde{T} = kT/\epsilon$, and $\tilde{p} = P\sigma^3/\epsilon$. Since the L-J parameters of Cl_2 are similar to those of xenon,[24] we may expect that the equation can be modified to describe diffusion of Cl_2 in xenon as well. Thus by substituting in eq 10 the geometric

(20) McCown, A. W.; Eden, J. G. *J. Chem. Phys.* **1984**, *81*, 2933.
(21) Grieneisen, H. P.; Jing, H. X.; Kompa, K. L. *Chem. Phys. Lett.* **1981**, *82*, 421.
(22) Marowsky, G.; Sauerbrey, R.; Tittel, F. K.; Wilson, W. L., Jr. *Chem. Phys. Lett.* **1983**, *98*, 167.
(23) See, for example, Zwanzig, R. W. *Phys. Rev. A* **1970**, *2*, 2005; *J. Chem. Phys.* **1974**, *60*, 4354.
(24) Hirschfelder, J. O.; Curtiss, C. F.; Bird, R. B. *Molecular Theory of Gases and Liquids*; Wiley: New York, 1954.
(25) Naghizadeh, J.; Rice, S. A. *J. Chem. Phys.* **1962**, *36*, 2710.
(26) Fajardo, M. E.; Apkarian, V. A.; Moustakas, A.; Krueger, H.; Weitz, E., submitted for publication in *J. Phys. Chem.*

mean of ϵ and the average of σ [ϵ(Xe) = 241 K, σ(Xe) = 4.07 Å, $\epsilon(Cl_2)$ = 357 K, $\sigma(Cl_2)$ = 4.11 Å], we may expect a reasonable description for the diffusion of Cl_2 in xenon. Furthermore, since the experiments are conducted along the saturated liquid–vapor coexistence line, a knowledge of T is sufficient for an accurate determination of P. An eight-term polynomial relating saturated vapor pressures of liquid xenon to temperature was given by Bearman et al.[15] The equation is accurate to within 3%. The temperature axis of Figure 3 can then be transformed to that of diffusion coefficient, D. A plot of k vs D is shown in Figure 4a. The data are well represented by linear fits with slopes:

$$dk/dD = 4\pi nr$$

A plot of the slopes versus n is shown in Figure 4b. The qualitative aspects of Figure 4 are the same as those of Figure 3 and its inset. As before, the data fit the model well; however, in this case r is obtained as 0.7 ± 0.1 Å. The implication is that the deactivation probability per encounter between exciplex and Cl_2 is ~0.1 (if we assume 7 Å as a reasonable hard-sphere diameter for Xe_2^+-Cl^-–Cl_2 collisions).

The same results are obtained when the activated model for viscosity, eq 7 and 8, is used with the explicit inclusion of the temperature dependence of viscosity. The plot of k vs $T/\eta(T)$ is not shown since it is indistinguishable from that of k vs D of Figure 4a. Following the same treatment as above, r/a = 0.16 ± 0.03 is obtained as the slope of the linear plot of $dk/d(T/\eta(T))$ vs n (see eq 7). If we use a = 4 Å, r = 0.65 ± 0.1 Å is obtained as the quenching radius. Thus two distinctly different treatments of the diffusive encounter model yield the same quenching cross section for $Xe_2^+Cl^-$ by Cl_2 in liquid xenon. The close agreement between these two analyses is because the derived quenching radii depend on the temperature dependence of the diffusion coefficients or viscosity and not on their absolute magnitudes.

It is worth comparing the liquid-phase data with those of the gas phase at room temperature. The deactivation of $Xe_2^+Cl^-$ by Cl_2 has been measured by several groups.[20-22] The results are, within a factor of 2, in agreement with each other. A reliable value for the quenching rate constant is 2.2 (±0.2) × 10^{-10} cm^3 s^{-1}, which corresponds to a quenching radius of 4.6 Å. Therefore the gas phase, room temperature deactivation efficiency by Cl_2 collisions is a factor of 6–7 larger. In the case of quenching by xenon collisions, the best known gas-phase value[20] is 6 × 10^{-15} cm^3 s^{-1}. This corresponds to ~3 × 10^5 gas kinetic collisions (using σ_{12} = 4.6 Å). If the same efficiency were maintained in the liquid phase, where the exciplex undergoes ~10^{13} collisions/s with the solvent atoms, the exciplex lifetime could not exceed 30 ns. Thus clearly, the liquid-phase deactivation probability due to collisions with xenon is significantly modified.

Finally, it is possible to comment on the role of Cl atoms in collisional or reactive quenching of the exciplex. Cl atoms are photogenerated in two different steps: in the photoinduced harpoon reaction of eq 1 and as a result of the radiative dissociation of the exciplex. In both cases hot Cl atoms are produced that could in principle deactivate the exciplex. This issue was not of relevance in xenon matrices since the Cl atoms are permanently dissociated and separated, as evidenced by the growth of exciplex emission intensity with irradiation time.[5] However, in the liquid phase and in the high-temperature solids, the halogen atoms recombine between pulses as verified by the absence of any growth in the exciplex emission intensity. Since the radiative lifetime of the exciplex is observed in the high-temperature solids and dilute liquids, it is to be concluded that the Cl atoms are ineffective in relaxing the exciplex and that the recombination to form the molecular halogens proceeds on the ground surface.

Conclusions

Emission spectra in gas, liquid, and solid xenon have been presented to clearly identify the nature of the emitter as Xe_2^+-$Cl^-(4^2\Gamma)$. The fluorescence lifetimes of $Xe_2^+Cl^-$ in solid and liquid xenon were reported. It was established that in the solids the exciplex relaxes radiatively at all temperatures. The radiative lifetime has a very mild temperature dependence throughout the studied range of densities and temperatures, τ_r = 225 ± 2 ns at 12 K and 240 ± 10 ns at 160 K, while it has previously been reported that in the gas phase[20] τ_r = 245 ± 10 ns. In the liquid phase, the only measurable nonradiative contribution to relaxation is due to $Xe_2^+Cl^-$–Cl_2 encounters. Two distinctly different models of diffusion-controlled encounters were used to reach the same conclusion; namely, the quenching efficiency of Cl_2 is 0.1–0.2 per encounter with the exciplex. In comparison with the gas phase it can be concluded that the deactivation probabilities with both xenon and Cl_2 are reduced in the liquids. This modification in collisional dynamics can perhaps be attributed to the strong interaction of the ionic exciplex state with the polarizable solvent atoms. Clustering of the exciplex with solvent atoms is to be expected. The large shift in emission spectra in the liquid phase, and the absence of a similar shift between low-temperature liquid and solid at 12 K, is a corroboration to this argument. The rigorous analysis of this specific solvent–solute interaction may provide a firmer basis for the interpretation of both dynamics and energetics.

Finally, while not as extensively studied, the results reported here are applicable to Xe_2Br and Xe_2F in liquid xenon and Kr_2F in liquid Kr. Namely, liquid-phase lifetimes comparable to those of the low-temperature solids, and therefore dominated by radiation, have been seen in all of these systems. Therefore, the result, liquid rare gases are ineffective in electronically relaxing exciplexes, seems to be general. The implications with respect to liquid-phase laser applications are obvious. Even at high molecular densities, there are no efficient radiationless deactivation channels in these solutions. Therefore, the successful design of liquid-phase rare gas halide lasers is reduced to the problem of devising efficient exciplex production schemes. The present scheme of two-photon cooperative optical pumping is particularly useful since it can be generalized to the entire family of rare gas halides.[13] The intermolecular charge-transfer transitions between xenon and X_2, where X_2 = F_2, Cl_2, and Br_2, in liquid xenon have recently been observed.[25] In all cases, an intense absorption that peaks near the UV cutoff (187 nm) of the spectrometer is observed. Thus efficient photoproduction of the xenon halides should be possible by the one-photon equivalent of the scheme presently used (eq 1) by pumping with ArF or KrF gas lasers.

Acknowledgment. We gratefully acknowledge the partial support of this research by the Research Corp. and the United States Air Force Astronautics Laboratory under Contract F04611-87-K-0024.

Registry No. $Xe_2^+Cl^-$, 67272-72-4; Xe, 7440-63-3.